New Journal of Physics
The open-access journal for physics

The trilinear Hamiltonian: a zero-dimensional model of Hawking radiation from a quantized source

Paul D Nation[1] **and Miles P Blencowe**
Department of Physics and Astronomy, Dartmouth College, Hanover, NH 03755, USA
E-mail: paul.d.nation@dartmouth.edu

New Journal of Physics **12** (2010) 095013 (18pp)
Received 7 April 2010
Published 30 September 2010
Online at http://www.njp.org/
doi:10.1088/1367-2630/12/9/095013

Abstract. We investigate a quantum parametric amplifier with dynamical pump mode, viewed as a zero-dimensional model of Hawking radiation from an evaporating black hole. We derive the conditions under which the spectrum of particles generated from vacuum fluctuations deviates from the thermal spectrum predicted for the conventional parametric amplifier. We find that significant deviations arise when the pump mode (black hole) has emitted nearly half of its initial energy into the signal (Hawking radiation) and idler (in-falling particle) modes. As a model of black hole dynamics, this finding lends support to the view that late-time Hawking radiation contains information about the quantum state of the black hole and is entangled with the black hole's quantum gravitational degrees of freedom.

[1] Author to whom any correspondence should be addressed.

Contents

1. Introduction

In the 35 years since Hawking's seminal paper on the quantum emission of radiation from a black hole [1], a large body of work has been devoted to solving the so-called information loss problem. For a black hole of fixed mass M, this emission process yields a black body spectrum with characteristic temperature $T_{\mathrm{H}} = \hbar c^3/8\pi k_{\mathrm{B}} GM$, irrespective of the initial state of the matter from which the black hole is formed. The inability to reconstruct the initial, possibly pure, state of the black hole from the total emitted radiation signals the apparent breakdown of unitary evolution and the S-matrix description of the Hawking process. Although Hawking's calculations have since been verified in a number of ways [2]–[6], this breakdown at the foundation of quantum mechanics suggests that our understanding of black hole dynamics is not yet complete.

The information loss problem rests on two key assumptions made in the standard derivation of Hawking radiation: (i) the perfectly thermal (i.e. mixed) character of the outgoing radiation; and (ii) the validity of this emission process over the lifetime of the black hole. The notion of a thermal spectrum considered here is not that of a blackbody frequency spectrum, but rather the quantum thermal probability distribution defined by the temperature T_{H} of a single mode (single frequency) of Hawking radiation. The traditional picture of the Hawking process leaves no room for deviations from this thermal distribution and thus breaks the requirement of pure-state→pure-state evolution enforced by unitarity. By itself, this process need not lead to information loss as the information content of the black hole may be stored in entanglement between particle pairs created on opposite sides of the horizon [7, 8]. Results from many-body theory suggesting that entanglement across a boundary scales with the area of the boundary lends credence to this view [9]. However, with the second assumption, the black hole causes a loss of entanglement and thus information.

With the expectation that information must be conserved, many suggestions for resolving the information loss problem have been put forward. Current proposed solutions include long-lived and stable Planck-scale remnants [10, 11], baby universes [12, 13] and the possibility of information escaping as non-thermal Hawking radiation [14, 15]. In all of these

proposals, corrections to the Hawking process manifest themselves when the black hole has evaporated to a size near that of the Planck length, $l_{\rm p} = \sqrt{\hbar G/c^3} \approx 10^{-35}$ m, at which quantum gravitational effects, neglected in Hawking's original analysis, are expected to play a role. In considering quantum states of the gravitational field, there is the possibility of backreaction and entanglement of the radiating matter degrees of freedom with those of gravity [16, 17]. Although it is natural to consider a quantized gravitational field for the Hawking process, the current lack of a full quantum mechanical description of gravity severely limits progress in addressing this scenario directly. In fact, exactly which degrees of freedom, if any, should be quantized is still a subject of debate [18, 19]. In this paper, we investigate a simple, zero-dimensional quantum optics model of Hawking radiation that mimics some of the essential physics present in the original information loss problem.

As a zero-dimensional model we consider the following trilinear Hamiltonian:

$$\hat{H} = \hbar\omega_a \hat{a}^+\hat{a} + \hbar\omega_b \hat{b}^+\hat{b} + \hbar\omega_c \hat{c}^+\hat{c} + \mathrm{i}\hbar\chi\left(\hat{a}\hat{b}^+\hat{c}^+ - \hat{a}^+\hat{b}\hat{c}\right), \tag{1}$$

consisting of three harmonic oscillator modes with the frequency relation, $\omega_a = \omega_b + \omega_c$. We designate the modes as pump ($\hat{a}$), signal ($\hat{b}$) and idler ($\hat{c}$), respectively. This Hamiltonian describes several quantum optics processes including frequency conversion, Raman and Brillouin scattering and the interaction of two-level atoms with a single mode resonant EM field and is the full quantum generalization of the parametric amplifier [20]–[27]. The connection between black hole radiance and parametric amplification was appreciated shortly after Hawking's discovery [28]. Both processes amplify vacuum fluctuations, resulting in the production of correlated photon pairs. Tracing over one of the two subsystems (i.e. signal and idler) yields statistics that are identical to those of a thermal distribution [29, 30]. The energy source in the parametric amplifier is assumed to be a classical pump, such as a laser or microwave generator with fixed amplitude driving a system with $\chi^{(2)}$ nonlinearity, the first nonlinear susceptibility in a medium without inversion symmetry [31]. Viewed as a black hole model, the pump plays the role of black hole mass M, while the signal and idler modes of the parametric amplifier represent the escaping and trapped Hawking photons, respectively, as depicted schematically in figure 1. The trilinear Hamiltonian (1) generalizes the parametric amplifier by quantizing the pump mode and allowing for energy loss to the signal and idler modes. The expectation value of the pump mode energy is analogous to the mass M of a quantum mechanical black hole. We explore this model by establishing the conditions under which the signal mode spectrum of the trilinear Hamiltonian deviates from the predicted thermal spectrum of the conventional parametric amplifier. We see that the quantization of the pump mode degree of freedom results, over time, in entanglement with the signal and idler modes and dynamics that become markedly different from the parametric approximation. In particular, the signal mode develops a strongly non-thermal spectrum that is dependent on the initial pump mode state. The corresponding entropy is reduced relative to that of a thermal (maximally mixed) state, indicating the presence of information. These model system results lend support to the view that late-time Hawking radiation contains an increasing amount of information about the initial quantum state of the black hole and is composed of particles entangled with quantized gravitational states.

The outline of this paper is as follows. In section 2, we review the derivation of the amplification of vacuum fluctuations under parametric approximation. Section 3 considers the semi-classical approximation whereby the backreaction from the quantized radiation onto the classical pump is accounted for and derives the self-consistent equations of motion

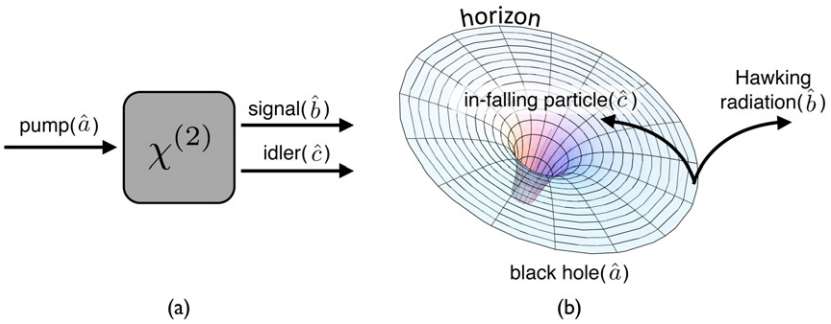

Figure 1. (a) Diagram depicting the dynamics of the trilinear Hamiltonian. Initial vacuum modes are not shown for clarity. The nonlinear interaction is generated by a system possessing a second-order susceptibility $\chi^{(2)}$. (b) Equivalent dynamical elements involved in the Hawking process.

for the signal and idler modes. In section 4, we consider the full quantum dynamics equation (1) under the short-time analytical approximation and compare this result, together with the full quantum numerical solution, to the parametric and semi-classical approximations from the previous sections. Section 5 investigates the role of entropy and entanglement in the production of non-thermal states. Finally, section 6 concludes with a brief discussion of the results and consequences for black hole evaporation.

2. The parametric amplifier and Hawking emission

In the following, we derive the well-known thermal spectrum of the signal mode under the parametric assumption of a fixed amplitude pump mode. Replacing the pump mode in equation (1) with a fixed amplitude drive A results in the interaction frame Hamiltonian

$$H_{\mathrm{I}} = \mathrm{i}\hbar\chi A\left(b^{+}c^{+} - bc\right). \tag{2}$$

The Heisenberg equations of motion for the signal and idler mode operators are

$$\frac{\mathrm{d}b(t)}{\mathrm{d}t} = A\chi c(t)^{+}; \quad \frac{\mathrm{d}c(t)}{\mathrm{d}t} = A\chi b(t)^{+}. \tag{3}$$

These can be readily solved yielding the Bogoliubov transformations

$$\begin{aligned} b(\tau) &= b(0)\cosh(A\tau) + c(0)^{+}\sinh(A\tau), \\ c(\tau) &= c(0)\cosh(A\tau) + b(0)^{+}\sinh(A\tau), \end{aligned} \tag{4}$$

where we have expressed the dynamics in dimensionless time $\tau = \chi t$. If the system starts with both signal and idler modes in the ground state, $|\Psi(0)\rangle = |0,0\rangle_{bc}$, then equation (4) gives, for the number operators N_b and N_c,

$$N_b(\tau) = N_c(\tau) = \sinh^2(A\tau). \tag{5}$$

Additionally, we are interested in the probability distribution of the individual signal and idler subsystems in the number state basis. With the system initially in the ground state, the unitary evolution corresponding to equation (2) can be expressed as

$$|\Psi(\tau)\rangle = \exp\left[A\tau\left(b^{+}c^{+} - bc\right)\right]|0,0\rangle_{bc}. \tag{6}$$

Making use of the disentangling theorem [32]

$$\exp\left[A\tau\left(b^{+}c^{+}-bc\right)\right]=\mathrm{e}^{\Gamma b^{+}c^{+}}\mathrm{e}^{-g\left(b^{+}b+c^{+}c+1\right)}\mathrm{e}^{-\Gamma bc}, \tag{7}$$

with $\Gamma=\tanh(A\tau)$ and $g=\ln\cosh(A\tau)$, where the last term in equation (7) vanishes for the ground state and the middle term reduces to e^{-g}, we have

$$\mathrm{e}^{\Gamma b^{+}c^{+}}\left|0,0\right\rangle_{bc}=\sum_{n=0}^{\infty}\frac{\Gamma^{n}\left(b^{+}c^{+}\right)^{n}}{n!}\left|0,0\right\rangle_{bc}=\sum_{n=0}^{\infty}\tanh^{n}(A\tau)\left|n,n\right\rangle_{bc}, \tag{8}$$

with the evolving state vector $|\Psi(\tau)\rangle$ given by

$$\left|\Psi(\tau)\right\rangle=\operatorname{sech}(A\tau)\sum_{n}\tanh^{n}(A\tau)\left|n,n\right\rangle_{bc}. \tag{9}$$

Let us now focus on operators acting on a subsystem spanned by the states of either the signal or idler mode individually. Assuming we are interested in the signal mode only, tracing over the idler subsystem in equation (9) gives the operator expectation value

$$\left\langle O(\tau)\right\rangle_{b}=\operatorname{sech}^{2}(A\tau)\sum_{n}\tanh^{2n}(A\tau)\left\langle n\right|O\left|n\right\rangle_{b} \tag{10}$$

for an arbitrary signal mode operator O. Comparing equation (10) with the spectrum of a thermal state defined by temperature T,

$$\left\langle O\right\rangle=\sum_{n}P_{n}\left\langle n_{b}\right|O\left|n_{b}\right\rangle=\left(1-\mathrm{e}^{-\hbar\omega_{b}/k_{\mathrm{B}}T}\right)\sum_{n}\mathrm{e}^{-n\hbar\omega_{b}/k_{\mathrm{B}}T}\left\langle n_{b}\right|O\left|n_{b}\right\rangle \tag{11}$$

indicates that the signal mode is in a thermal state provided that we define the temperature as

$$T\left(\tau\right)=\frac{\hbar\omega_{b}}{2k_{\mathrm{B}}\ \ln\left[\coth(A\tau)\right]}, \tag{12}$$

where the time dependence is a consequence of the rapid increase in the occupation number of the modes, equation (5). As in the Hawking process [33], the particle pairs generated by the parametric amplifier form an entangled two-mode squeezed state given by equation (9) [34]. The bipartite structure of this system allows calculating the entanglement between particle pairs via the von Neumann entropy S_i, also referred to as entanglement entropy. For mode $i=b,c$, using the reduced density matrix ρ_i, we have

$$S_{i}=-\mathrm{Tr}\left(\rho_{i}\ \ln\ \rho_{i}\right), \tag{13}$$

where we drop the usual k_{B} factor. For both the signal and idler modes, this entropy is given by

$$S^{\mathrm{th}}=-\ln\left[1-\mathrm{e}^{-\hbar\omega/k_{\mathrm{B}}T(\tau)}\right]-\frac{\hbar\omega}{k_{\mathrm{B}}T(\tau)}\left[1-\mathrm{e}^{\hbar\omega/k_{\mathrm{B}}T(\tau)}\right]^{-1}, \tag{14}$$

which is the thermal entropy of a quantum harmonic oscillator with temperature defined by equation (12). Thus, as for the Hawking thermal radiation, we see that the temperature of the parametric oscillator is determined by the entropy generated from tracing over one of the two modes in a particle pair squeezed state.

3. Semi-classical analysis: backreaction on a classical pump mode

We now go beyond the just-considered parametric amplifier model and incorporate backreaction effects due to the emission process using a semi-classical approximation where the pump mode is treated as a classical variable, while the signal and idler modes are quantized. In order to self-consistently solve for the system evolution, we first work out the dynamics of the pump mode, assuming it behaves as a classical variable affected by the expectation values of the signal and idler modes, after which we substitute the resulting c-number expressions for the pump operators into the Hamiltonian and calculate the signal and idler evolution. A similar procedure arises for the semi-classical Einstein equations:

$$G_{\mu\nu} = \frac{8\pi G}{c^4}\left\langle \Psi|\hat{T}_{\mu\nu}|\Psi\right\rangle, \tag{15}$$

where the mass M black hole spacetime geometry is modeled classically through the usual Einstein tensor $G_{\mu\nu}$, interacting with the quantum matter/radiation fields via the expectation value of the stress–energy–momentum tensor operator $\hat{T}_{\mu\nu}$ with respect to a suitable incoming quantum field state $|\Psi\rangle$. Solving these semiclassical equations using an analogous procedure to that outlined above yields a nonlinear Schrödinger equation [35] and also a possible loss of spacetime stability [36]. In addition, issues such as non-causal dynamics [37] and possible inconsistencies with wavefunction collapse [38] occur. In contrast, the semi-classical model presented here can be readily solved by exploiting the symmetries present in the Hamiltonian.

To begin, we consider equation (1) in the interaction frame,

$$H_I = \mathrm{i}\hbar\chi\left(ab^+c^+ - a^+bc\right) \tag{16}$$

and obtain the following mode equations:

$$\frac{\mathrm{d}a}{\mathrm{d}t} = -\chi bc, \quad \frac{\mathrm{d}b}{\mathrm{d}t} = \chi ac^+, \quad \frac{\mathrm{d}c}{\mathrm{d}t} = \chi ab^+ \tag{17}$$

that lead to the evolution of the pump mode number operator,

$$\frac{\mathrm{d}N_a}{\mathrm{d}t} = -\chi\left(ab^+c^+ + a^+bc\right). \tag{18}$$

It is easy to show that the corresponding number operators for signal and idler modes are given by $\mathrm{d}N_b/\mathrm{d}t = \mathrm{d}N_c/\mathrm{d}t = -\mathrm{d}N_a/\mathrm{d}t$. To proceed, we will use the following Manley–Rowe constants of motion [39]:

$$M_{ab} = N_a + N_b, \quad M_{ac} = N_a + N_c, \quad M_{bc} = N_b - N_c, \tag{19}$$

expressing the underlying SU(2) and SU(1,1) symmetries in our model [40, 41]. Differentiating equation (17) again results in decoupled equations of motion containing only commuting operators:

$$\begin{aligned}
\frac{\mathrm{d}^2N_a}{\mathrm{d}t^2} &= 2\chi^2\left[3N_a^2 - N_a\left(2M_{ab} + 2M_{ac} + 1\right) + M_{ab}M_{ac}\right],\\
\frac{\mathrm{d}^2N_b}{\mathrm{d}t^2} &= -2\chi^2\left[3N_b^2 - N_b\left(4M_{ab} - 2M_{ac} - 1\right) + M_{ab}\left(M_{ab} - M_{ac} - 1\right)\right],\\
\frac{\mathrm{d}^2N_c}{\mathrm{d}t^2} &= -2\chi^2\left[3N_c^2 - N_c\left(4M_{ac} - 2M_{ab} - 1\right) + M_{ac}\left(M_{ac} - M_{ab} - 1\right)\right].
\end{aligned} \tag{20}$$

We now take the expectation value of the pump number operator equation (20) for N_a and make the approximation $\langle N_a^2\rangle \approx \langle N_a\rangle\langle N_a\rangle$, the validity of which can be checked using full quantum numerical simulations of equation (17) (see section 4). These approximations, along with the condition that both signal and idler mode start in the vacuum state, lead to the semiclassical evolution for the pump mode:

$$N_a(\tau) = \beta_+ + [N_a(0) - \beta_+]\,\mathrm{dn}\left[\sqrt{\beta_+ - \beta_-}\,\tau,\ \frac{N_a(0) - \beta_-}{\beta_+ - \beta_-}\right]^{-2}, \tag{21}$$

where $\mathrm{d}n(u, k)$ is the Jacobi elliptic function and

$$\beta_\pm = \frac{1}{4}\left[1 + 2N_a(0) \pm \sqrt{1 + 12N_a(0) + 4N_a(0)^2}\right]. \tag{22}$$

It is important to note that both equations (21) and (22) are expressed in terms of the initial conditions of the pump mode only, a consequence of relations (19) and the fact that the signal and idler are initially in the vacuum (ground) state. Equations of motion for both the signal and idler can then be obtained by the substitution of the c-number expressions for the pump mode with amplitude given by equation (21),

$$a = \sqrt{N_a(\tau)}\mathrm{e}^{-\mathrm{i}\phi(t)}, \quad a^+ = \sqrt{N_a(\tau)}\mathrm{e}^{\mathrm{i}\phi(t)}, \tag{23}$$

where $\phi(t)$ is a slowly varying function of time, into equation (16):

$$\tilde{H}_\mathrm{I} = \mathrm{i}\hbar\chi N_a(t)^{1/2}\left(b^+c^+\mathrm{e}^{-\mathrm{i}\phi(t)} - bc\mathrm{e}^{\mathrm{i}\phi(t)}\right). \tag{24}$$

The time evolution of this now bilinear Hamiltonian can be calculated straightforwardly if we assume that [25]

$$\sqrt{N_a(t)}\frac{\mathrm{d}\phi(t)}{\mathrm{d}t} = \mathrm{const}, \tag{25}$$

which is the most general condition under which the Hamiltonian at different times commutes, $[\tilde{H}_\mathrm{I}(t), \tilde{H}_\mathrm{I}(t')] = 0$. Combining equations (17) and (23) results in the phase relation

$$a^+\frac{\mathrm{d}a}{\mathrm{d}t} - a\frac{\mathrm{d}a^+}{\mathrm{d}t} = -2\mathrm{i}N_a\frac{\mathrm{d}\phi(t)}{\mathrm{d}t}, \tag{26}$$

which, expressing the left-hand side as equation (16) through the Heisenberg equations for the operators equation (17), yields a second condition for the pump phase:

$$2N_a(t)\frac{\mathrm{d}\phi(t)}{\mathrm{d}t} = \langle\tilde{H}_\mathrm{I}\rangle. \tag{27}$$

As long as the initial state contains at least one mode in the vacuum state, we have the constant of motion $\langle H_I\rangle = 0$. Thus, equations (25) and (27) are only consistent if $\phi(t) = 0$. This leads to a bilinear Hamiltonian of the form,

$$\tilde{H}_\mathrm{I} = \mathrm{i}\hbar\chi N_a(t)^{1/2}\left(b^+c^+ - bc\right). \tag{28}$$

Using a similar analysis to that employed in section 2 gives

$$\begin{aligned}\frac{\mathrm{d}b(\tau)}{\mathrm{d}\tau} &= b(0)\cosh(\theta(\tau)) + c^+(0)\sinh(\theta(\tau))\\ \frac{\mathrm{d}c(\tau)}{\mathrm{d}\tau} &= c(0)\cosh(\theta(\tau)) + b^+(0)\sinh(\theta(\tau)),\end{aligned} \tag{29}$$

where

$$\theta(\tau) = \int_0^\tau \sqrt{N_a(\tau')}\,\mathrm{d}\tau'. \tag{30}$$

Therefore, we see that each mode behaves similarly, as in the parametric approximation, but with the number of particles dependent on the pump dynamics:

$$N_b(\tau) = N_c(\tau) = \sinh^2(\theta(\tau)). \tag{31}$$

However, and most importantly, the modes are again in a thermal state with distribution

$$\langle O(\tau)\rangle = \operatorname{sech}^2\left(\sqrt{N_a(\tau)}\tau\right)\sum_n \tanh^{2n}\left(\sqrt{N_a(\tau)}\tau\right)\langle n|O|n\rangle. \tag{32}$$

Thus, the spectrum of the signal mode (Hawking radiation) remains thermal when pump mode energy loss due to signal and idler particle creation is taken into account within the semi-classical approximation.

4. Full quantum description

4.1. Short-time approximation

In this section, we consider the full quantum dynamics of the trilinear Hamiltonian equation (1) (i.e. quantize the pump mode as well). Although the trilinear system does not allow for a general analytical solution, we can obtain approximate equations in the short-time limit $\tau = \chi t \ll 1$. Using the condition $\omega_b = \omega_c = \omega_a/2$, appropriate for modeling particle generation by a black hole, we can rewrite equation (1) ignoring constant terms as

$$H = H_0 + H_{\mathrm{int}} = \hbar\omega_a\left(a^+a + K_z\right) + \mathrm{i}\hbar\chi\left(aK_+ - a^+K_-\right), \tag{33}$$

where

$$K_+ = b^+c^+, \quad K_- = bc, \quad K_z = \tfrac{1}{2}\left(b^+b + c^+c + 1\right). \tag{34}$$

We now construct the Casimir operator

$$K^2 = K_z^2 - \tfrac{1}{2}\left(K_+K_- + K_-K_+\right) = \tfrac{1}{4}\left(M_{bc}^2 - 1\right), \tag{35}$$

where the second equality comes from definition (19). This operator obeys the eigenvalue equation

$$K^2|\Psi\rangle = k(k-1)|\Psi\rangle, \tag{36}$$

where $k = 1/2(|M_{bc}| + 1)$. We now look for simultaneous eigenstates of both K^2 and K_z: $|k, n_c\rangle$, where n_c is the number of idler particles. These states can also be decomposed using the number state basis

$$|k, n_c\rangle = |n_c + 2k - 1\rangle_b\,|n_c\rangle_c = |n_b\rangle\,|n_c\rangle, \tag{37}$$

with n_b representing the number of particles in the signal. Operating on this state with K_z gives

$$K_z|k, n_c\rangle = (k + n_c)|k, n_c\rangle = \left(\frac{n_b + n_c + 1}{2}\right)|n_b\rangle\,|n_c\rangle, \tag{38}$$

valid only for initial conditions where both the signal and idler modes are in pure states satisfying $n_b \geqslant n_c$. Including the pump mode state in the full state vector and expressing the idler mode population as a function of the pump amplitude

$$|n_a\rangle\,|k,\, M_{ac} - n_a\rangle\,, \tag{39}$$

one may switch to the interaction frame where the evolution depends only on $H_{\rm int}$ (33)

$$|\tau;\, k,\, M_{ac}\rangle = \mathrm{e}^{\tau\left(aK_+ - a^+K_-\right)}\,|0;\, k,\, M_{ac}\rangle, \tag{40}$$

where the initial state with $M_{ac} = N_a(0)$ is given by

$$|0;\, k,\, M_{ac}\rangle = |M_{ac}\rangle\,|k,\, 0\rangle\,. \tag{41}$$

The short-time approximation $\tau = \chi t \ll 1$ to equation (40) can be calculated using the Baker–Campbell–Hausdorff (BCH) formula truncated to $O(\tau^2)$

$$\mathrm{e}^{\tau\left(aK_+ - a^+K_-\right)} \approx \mathrm{e}^{\tau aK_+}\mathrm{e}^{-\tau a^+K_-}\mathrm{e}^{-\tau^2/2\left[aK_+,\,a^+K_-\right]}. \tag{42}$$

Acting with the third exponential operator term on our initial state gives

$$\mathrm{e}^{-\tau^2/2\left[aK_+,\,a^+K_-\right]}|M_{ac}\rangle|k,\,0\rangle \approx \left(1 - kM_{ac}\tau^2\right)|M_{ac}\rangle|k,\,0\rangle, \tag{43}$$

indicating clearly that the time over which the approximation is valid $t = \tau/\chi < 1/(\chi\sqrt{kM_{ac}})$ decreases with pump amplitude and coupling strength. Evaluating the BCH approximated expression (42) on the initial state (41), we obtain for the full evolution of the state:

$$|\tau;\, k,\, M_{ac}\rangle = \frac{1}{\sqrt{N_{M_{ac}}(\tau)}}\sum_{n=0}^{M_{ac}} f_n\,(k,\, M_{ac})\,\tau^n|M_{ac} - n\rangle|k,\, n\rangle, \tag{44}$$

where $N_{M_{ac}}(\tau)$ is the time-dependent normalization factor

$$N_{M_{ac}}(\tau) = \mathrm{e}^{\tau^{-2}}\tau^{2M_{ac}}\Gamma\left(M_{ac}+1,\,\tau^{-2}\right), \tag{45}$$

with $\Gamma(a,\,b)$ being the reduced gamma function and

$$f_n\,(k,\, M_{ac}) = \left[\frac{M_{ac}!\Gamma\,(2k+n)}{n!\,(M_{ac}-n)!\Gamma\,(2k)}\right]^{1/2}. \tag{46}$$

Our interest in the crossover from classical to quantum dynamics for the pump mode suggests that we use coherent states built from linear combinations of equation (44) for the initial pump state. To this end, we consider a general initial state

$$|\Psi(0)\rangle = \sum_{s=0}^{\infty} a_s\frac{f_0(s)}{\sqrt{N_s(0)}}|s\rangle|0\rangle|0\rangle, \tag{47}$$

with the pump mode in an as yet unspecified initial pure state with probability $P_{\rm s} = |a_{\rm s}|^2$ of being in state s and both signal and idler modes in the vacuum state ($k = 1/2$). Here we implicitly assume the probabilities are normalized and add to unity. The density matrix at some later time τ resulting from (47) is given by

$$\rho^{\Psi}_{abc}(\tau) = \sum_{s=0}^{\infty}\sum_{r=0}^{\infty}\sum_{i=0}^{s}\sum_{j=0}^{r} a_s a_r^*\frac{f_i(s)\tau^i}{\sqrt{N_s(\tau)}}\frac{f_j(r)\tau^j}{\sqrt{N_r(\tau)}}|s-i\rangle|i,\,i\rangle\langle r-j|\langle j,\,j|, \tag{48}$$

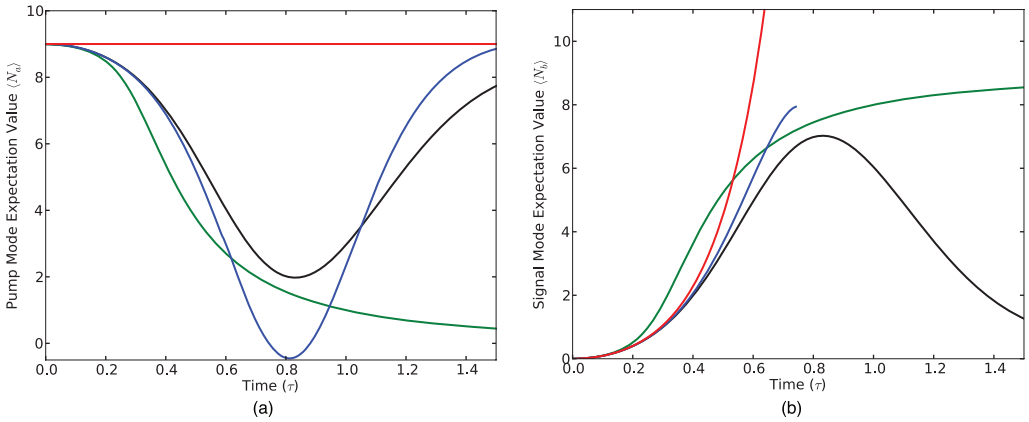

Figure 2. (a) Evolution of pump mode initially in coherent state $\langle N_a(0)\rangle = 9$ for the parametric (red), semi-classical (blue), short-time quantum approximation (green), and full quantum numerical solution (black), as a function of dimensionless time $\tau = \chi t$. (b) Corresponding population of the signal mode. Note that the semi-classical analysis ceases to be valid when the pump mode becomes depleted.

which, after performing a partial trace, leads to the reduced density operators

$$\rho_a^{\Psi}(\tau) = \sum_{s=0}^{\infty}\sum_{r=0}^{\infty}\sum_{i=0}^{s}\sum_{j=0}^{r} a_s a_r^* \frac{f_i(s)\tau^i}{\sqrt{N_s(\tau)}}\frac{f_j(r)\tau^j}{\sqrt{N_r(\tau)}}\delta_{i,j}|s-i\rangle\langle r-j|, \tag{49}$$

where $\delta_{i,j}$ is the Kronecker delta, and

$$\rho_b^{\Psi}(\tau) = \sum_{s=0}^{\infty}\sum_{i=0}^{s} P_s \frac{f_i^2(s)}{N_s(\tau)}\tau^{2i}|i\rangle\langle i| \tag{50}$$

for the pump and signal modes, respectively. Figure 2 compares the expectation values of the pump and signal modes for the parametric, semi-classical and short-time quantum approximations, as well as the full numerical solution to equation (17), where the pump mode is initially in a coherent state with amplitude $\langle N_a(0)\rangle = 9$ corresponding to classical pump modes with amplitude $A = 3$, and the signal and idler modes are initially in their vacuum (ground) states.

4.2. Mode spectrum dynamics under the short-time approximation

The main limitation of the short-time approximation is its inability to account for backreaction effects resulting from the build-up of quanta in the signal and idler modes. For particles produced in the Hawking process, however, the entangled pairs generated early in the evolution do not, to first-order, affect those created later from the black hole [42]. Furthermore, the emitted radiation does not build up in the vicinity of the black hole, but escapes to spatial infinity. Therefore, in this section we will suppose that the expressions derived above for the evolving pump and signal states, equations (49) and (50) respectively, in fact provide a more relevant zero-dimensional model of a radiating blackhole when extrapolated beyond their original short-time domain of validity. The pump and signal modes contain in general a large number

of coefficients for each number state and cannot be easily evaluated. However, in the long-time limit where the pump is nearly depleted, these equations can be considerably simplified by noting that a general element of equation (50) for fixed s is given by

$$P_{\mathrm{s}}\frac{f_i^2(s)}{N_s(\tau)}\tau^{2i} = P_{\mathrm{s}}\frac{\mathrm{e}^{-\tau^{-2}}}{u!\tau^{2u}}\frac{\Gamma(s+1)}{\Gamma\left(s+1,\tau^{-2}\right)}, \quad u = s-i. \tag{51}$$

As such, only those elements where $i = s$ remain nonzero, leading to the signal mode density matrix

$$\rho_b^{\Psi} = \sum_{s=0}^{\infty} P_{\mathrm{s}}|s\rangle\langle \mathrm{s}|, \tag{52}$$

which is in general a mixed state with number-state probability distribution P_s identical to that of the initial pump state. Therefore, by measuring the late-time signal or idler mode distribution we recover all but the phase information associated with the initial pure state of the pump mode. Additionally, equation (52) shows that the number of quanta in the signal mode is equal to the initial number of quanta in the pump mode, indicating that the pump (49) ends up in the vacuum (ground) state.

The most important knowledge gained from equation (52) is that the signal mode spectrum will no longer be that of a thermal state, in contrast to the parametric and semi-classical approximations in sections 2 and 3, respectively. Focusing on coherent states, in figure 3 we give an example of the evolution of equations (49) and (50) by plotting the probability distributions for both modes as a function of time τ for a pump initially in a coherent state with amplitude $\langle N_a(0)\rangle = 9$ and initial vacuum state for both the signal and idler. Additionally, in figure 3(b) we highlight what the thermal distribution would be at each time step by equating $\langle N_b(\tau)\rangle$ with a Bose–Einstein distribution to extract an effective temperature

$$\langle N_b(\tau)\rangle = \left[\mathrm{e}^{\hbar\omega_b/k_{\mathrm{b}}T_{\mathrm{eff}}(\tau)} - 1\right]^{-1}. \tag{53}$$

In figure 3(a), we see the evolution of the initial coherent state as it loses quanta to the signal and idler modes and evolves towards the ground state represented by a peak in the probability distribution at the $n = 0$ number state. The corresponding evolution of the signal mode in figure 3(b) starts with the vacuum state and progresses towards the state with probability distribution identical to that of the initial pump coherent state, equation (52). By comparison with the effective thermal state (53), we can see that the initial probability distribution for the signal mode is nearly that of a thermal state until the pump mode has transferred nearly half of its initial energy corresponding to $\langle N_b(\tau)\rangle = 4.5$. As the evolution continues, figure 3(b) shows the increasing deviation from the effective thermal description for the signal mode distribution as expected from equation (52).

4.3. Non-thermal spectra and information

We now quantify the deviations of the signal mode spectrum equation (50) from that of a thermal state using the fidelity [43]

$$F_b(\tau) = \mathrm{Tr}\sqrt{\rho_b(\tau)^{1/2}\sigma(\tau)\rho_b(\tau)^{1/2}}, \tag{54}$$

where $\rho_b(\tau)$ is the density matrix of the signal mode and $\sigma(\tau)$ is a thermal density matrix with effective temperature determined by equation (53) using the occupation number $\langle N_b(\tau)\rangle$. The

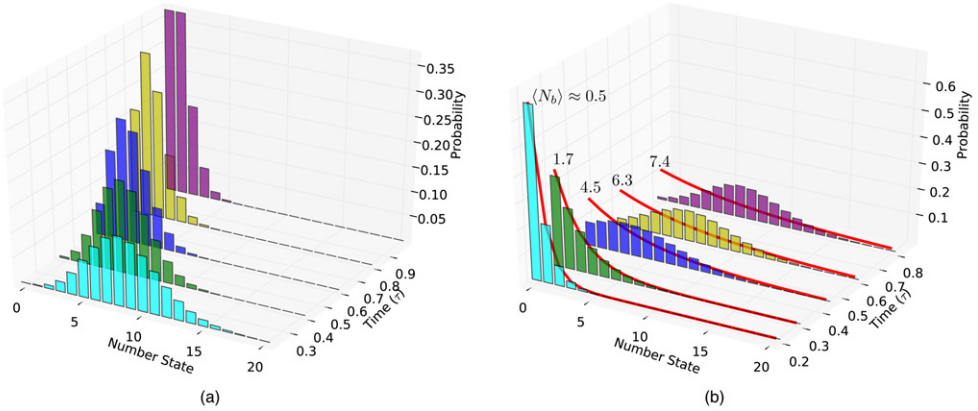

Figure 3. (a) The spectrum of the pump mode at several timesteps when the pump is initially in a coherent state with $\langle N_a(0)\rangle = 9$. (b) The corresponding spectrum of the signal mode. Red lines indicate what the distribution would be at each timestep if in a thermal state corresponding to occupation number $\langle N_b(\tau)\rangle$, equation (53).

fidelity provides a measure of the distance between these two states in distribution space with range $0 \leqslant F \leqslant 1$, where unity indicates that the two density matrices are identical. In figure 4(a), we plot the fidelity of the signal mode assuming a pump mode initially in a coherent state starting with several occupation numbers ranging from 1 to 9. By comparison with figure 2, we can see that for the initial coherent state $\langle N_a(0)\rangle = 9$, the fidelity remains essentially unity, indicating that the signal mode density matrix equation (50) is nearly thermal until the pump has transferred close to half of its initial energy into the signal and idler modes, beyond which point there is a strong deviation from the thermal state as the signal mode asymptotically approaches the state given by equation (52). This is in agreement with the qualitative description presented in figure 3(b) and remains true for all the initial states considered in figure 4(a).

This deviation from a thermal distribution also indicates that the signal mode spectrum contains information defined as [14]

$$I_b(\tau) = S_b^{\text{th}}(\tau) - S_b(\tau), \tag{55}$$

where $S_b^{\text{th}}(\tau)$ is the von Neumann entropy of the signal mode in a thermal state with equal average occupation number, equation (14), and $S_b(\tau)$ is the actual entropy of the mode calculated using equation (13) and the reduced density matrix of the signal mode $\rho_b(\tau)$. In figure 4(b) we plot the information contained in the signal mode for the initial pump coherent states considered in figure 4(a). Given that the fidelity is nearly unity until the pump mode transfers half of its original quanta to the signal and idler modes, it follows that the information content of the signal or idler mode is close to zero over the same time interval before increasing as the signal spectrum becomes identical to that of the initial coherent states.

In order to account for the dynamics of the signal mode information, we first consider a general bipartite pure state of a system with fixed total energy that is composed of subsystems A and B, each with finite Hilbert space dimensions d_{A} and d_{B}, respectively. It is known that subsystem B will be nearly thermal and thus contain approximately no information as long as $d_{\text{A}} \gg d_{\text{B}}$, with the information content of subsystem B becoming apparent only after $d_{\text{A}} \approx d_{\text{B}}$ [14, 44, 45]. Similar dynamics for the information content of the signal mode is shown

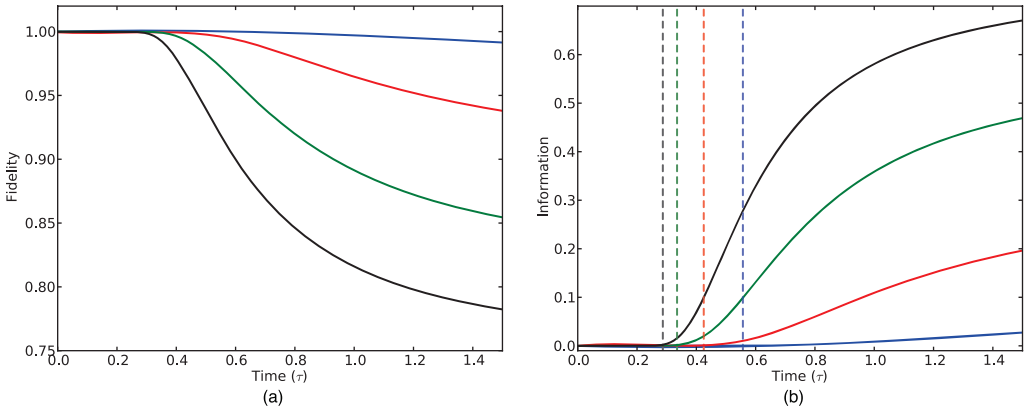

Figure 4. (a) Fidelities of the signal mode given a pump mode initially in a coherent state with occupation number $\langle N_a \rangle = 1$ (blue), 3 (red), 6 (green) and 9 (black) under the short-time approximation. b) Information present in the signal spectrum calculated from equation (55). Equivalently colored vertical lines denote the time at which the effective subspace dimensions satisfy, $d_a^{\text{eff}} = d_{bc}^{\text{eff}}$.

in figure 4. However, the three Harmonic oscillator modes from which a pure state of the trilinear Hamiltonian equation (1) is composed all contain an infinite set of states, preventing the direct application of dimensional arguments to our model. One can, however, define an effective subspace dimension for each mode [45]

$$d_i^{\text{eff}}(\tau) = \frac{1}{\text{Tr}\left[\sigma_i^2(\tau)\right]}, \quad i = a, b, c \tag{56}$$

determined by the purity of the effective thermal state $\sigma_i(\tau)$, with the temperature given by equation (53). This definition is motivated by the fact that the purity of a mixed state density matrix is proportional to the number of basis states over which the fractional population of the mixed state is nonzero. For a state with an energy (quanta) constraint, using the thermal state $\sigma(\tau)$ gives the minimal value for the purity, and as such equation (56) represents an effective maximum number of states constrained by the number of quanta in the mode at time τ. Therefore, if we partition our initial pure state into bipartite subsystems d_a and d_{bc} composed of pump and combined signal and idler modes, respectively, then the initial effective subspace dimensions satisfy $d_a^{\text{eff}} \gg d_{bc}^{\text{eff}} = (d_b^{\text{eff}})^2$, where the equality is due to the symmetry between the signal and idler modes. In figure 4(b), we plot the times at which $d_a^{\text{eff}} = d_{bc}^{\text{eff}}$ for each of the initial pump mode coherent states considered in figure 4(a). Just as for finite dimensional pure states, the information contained in the signal or idler subsystems remains nearly zero until after $d_a^{\text{eff}}(\tau) \approx d_{bc}^{\text{eff}}(\tau)$, provided we define the effective subspace dimension using equation (56). Our results are in agreement with those of Page [14] where a similar argument was put forth for the evolution of information in the Hawking radiation from a finite-dimensional black hole.

4.4. Numerical results for the full trilinear evolution

Unlike Hawking radiation, which is well modeled using the quantum short-time approximation, backaction due to the build-up of quanta in the signal and idler modes has a strong effect on the evolution of the trilinear Hamiltonian (16). In figure 2, we see that backreaction effects quickly

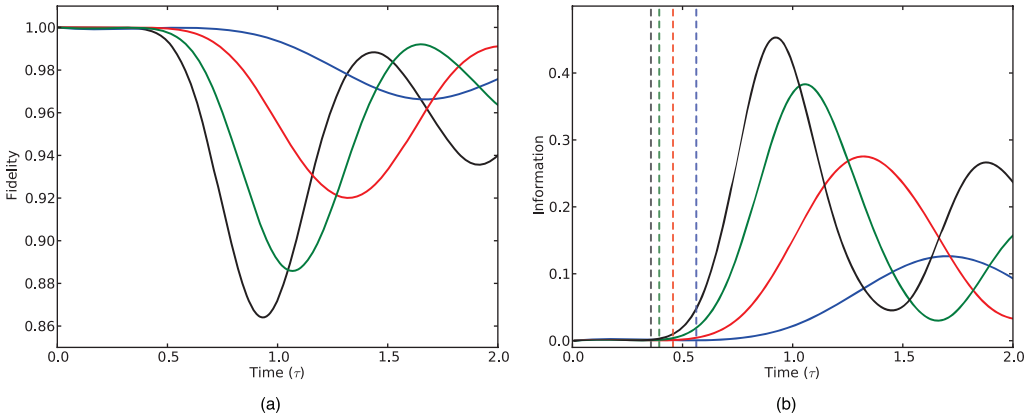

Figure 5. (a) Fidelities of the signal mode using numerical simulations of equation (17) with a pump mode initially in a coherent state with occupation number $\langle N_a \rangle = 1$ (blue), 3 (red), 6 (green) and 9 (black). (b) The corresponding information present in the signal mode spectrum and times at which $d_a^{\text{eff}}(\tau) = d_{bc}^{\text{eff}}(\tau)$ (dashed lines).

lead to differing evolutions between the short-time and full quantum dynamics; backreaction prevents the full transfer of quanta from the pump mode [46] and results in the oscillation of quanta between the pump and signal/idler modes. To account for these backaction terms we repeat the analysis in section 4.3 by numerically calculating the full dynamics of equation (17). Figure 5 shows the modifications to both the fidelity and information content of the signal mode when backaction is included in the dynamics, as well as the subspace dimension condition $d_a^{\text{eff}}(\tau) = d_{bc}^{\text{eff}}(\tau)$. As expected, the short-time dynamics in figure 5 are nearly identical to those in figure 4 until $d_a^{\text{eff}}(\tau) \approx d_{bc}^{\text{eff}}(\tau)$, which occurs later than in the short-time approximation as the backaction from particles in the signal mode begins to impede the transfer of quanta from the pump. The peaks in the information content of the signal mode correspond to the times at which backaction from the pump mode has completely stopped the transfer of energy between modes. With the majority of quanta now in the signal and idler modes, the flow of energy reverses directions as the signal and idler now drive the pump mode, leading to the oscillations seen in figure 5. As a model for black hole evaporation these oscillations represent the unphysical process of Hawking radiation flowing back into the black hole; the connection between the trilinear Hamiltonian and Hawking emission is valid only for the initial transfer of quanta from pump to signal/idler modes.

5. Tripartite entanglement

With the pump mode quantized, one can consider the entanglement between the pump and signal/idler modes. In section 2, it was shown that ignoring this entanglement (pump mode treated classically) and tracing over one mode of a two-mode squeezed state lead directly to the thermal characteristics of the remaining system. In the full quantum description, the statistics of the signal mode is obtained by tracing over both idler and pump modes and, as such, the distribution of entanglement between modes of this now tripartite system is important for characterizing the spectrum of the signal mode. Additionally, entanglement with the pump mode

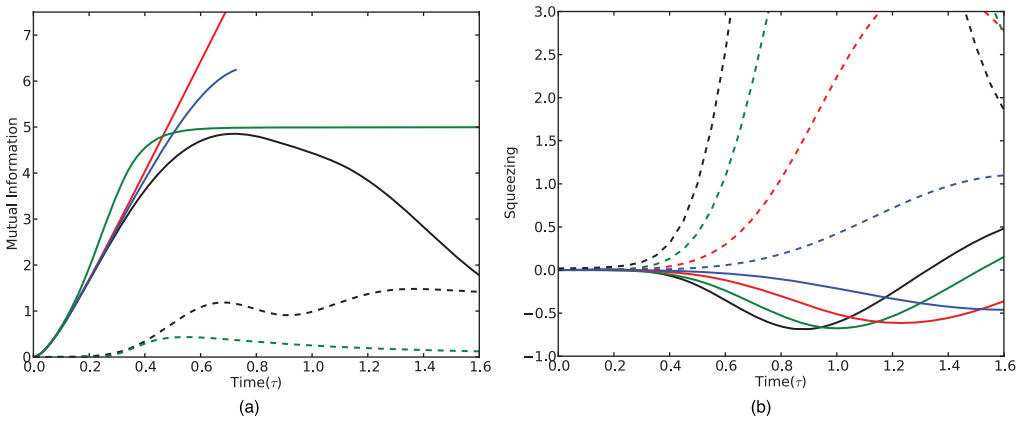

Figure 6. (a) Signal–idler mutual information I_{b-c} for a pump with $\langle N_a(0)\rangle = 9$ in the parametric (red), semi-classical (blue), quantum short-time (green) and full numerical solution (black). Dashed lines represent mutual information I_{a-bc}, indicating entanglement with the pump mode. (b) Quadrature squeezing parameters $q_\pm$ of the pump mode given the pump is initially in a coherent state with occupation number $\langle N_a\rangle = 1$ (blue), 3 (red), 6 (green) and 9 (black). Negative values indicating squeezing of the q_- quadrature. Dashed lines represent the corresponding q_+ quadrature.

may appreciably alter the state dynamics of the pump compared to the classical approximations in sections 2 and 3. Given that multipartite entanglement is not as well understood as for the bipartite case, we begin by again considering the system to be partitioned into two subsystems, consisting of the pump mode and the combined signal–idler. This bipartite separation into pump and signal–idler subsystems allows us to use the mutual information [43]

$$I_{a-bc} = S_a + S_{bc} - S_{abc} \tag{57}$$

as a measure of total correlations, both classical and quantum, between subsystems [47]. Since our tripartite system state remains pure throughout its evolution, the total entropy $S_{abc} = 0$ and the subsystem entropies satisfy $S_a = S_{bc}$. The mutual information is therefore twice the entropy of the pump mode subsystem, $I_{a-bc} = 2S_a$. Thus, the subsystem entropy of the pump is a direct measure of entanglement with the signal and idler modes, which is not taken into account in either the parametric or semi-classical solutions. Of course the signal and idler subsystems are also entangled with each other as in sections 2 and 3. With both signal and pump modes in identical states, the signal–idler mutual information is given by

$$I_{b-c} = S_b + S_c - S_{bc} = 2S_b - S_a, \tag{58}$$

indicating the tradeoff between the entanglement of the signal/idler and that of the pump mode equation (57). In figure 6(a), we plot the mutual information equations (57) and (58) for a pump initially in a coherent state of amplitude $\langle N_a(0)\rangle = 9$ for the parametric, semi-classical and short-time approximations along with the full numerical solution obtained using equation (17). We see that the mutual information (pump entanglement) I_{a-bc} begins to become appreciable around the same time as the information content of the signal mode becomes apparent in figures 4(b) and 5(b), indicating the increasing role of the pump mode in the dynamics. The numerical solution shows that this increase in pump entanglement reduces the signal–idler

mutual information I_{b-c} with respect to the semi-classical and parametric approximations, as expected from equation (58). In the full quantum dynamics the pump is never allowed to be fully depleted and is therefore always entangled with the signal and idler. However, in the short-time approximation, the late-time pump mode is depleted and approaches the ground state where $S_a = 0$.

Finally, we show that the entanglement build-up with the pump mode given by I_{a-bc} not only affects the signal and idler modes, but also results in amplitude-dependent squeezing of the pump. In figure 6(b), we plot the amplitude of the squeezing parameters [34]

$$q_{\pm} = 4\left\langle \Delta X_{\pm}^2 \right\rangle - 1, \quad X_{\pm} = \frac{a(\tau) \pm a^{+}(\tau)}{2} \tag{59}$$

for the pump mode, where $\langle \Delta X_{\pm}^2 \rangle$ is the variance of the quadratures. As can be seen, the entanglement with the signal and idler modes leaves the pump mode in a non-classical squeezed state over the time range of interest.

6. Conclusion

In this paper, we have investigated the effect of a dynamical quantized pump mode on the generation of quanta in a parametric amplifier. We have shown that a quantized pump mode leads naturally to a non-thermal spectrum for the signal and idler modes once the pump has released nearly half of its initial energy, such that the effective subspace dimensions of the pump and signal/idler mode systems approximately coincide. The departure from a thermal state indicates that the signal spectrum contains information that may be used to partially reconstruct the initial state of the pump mode. Once quantized, the pump mode becomes entangled with the signal and idler, leading to non-classical squeezed states of the pump. As a simple, zero-dimensional model of the Hawking effect, the present findings lend support to the possibility of non-thermal emission from a quantum (as opposed to semiclassical) black hole; the emitted radiation is entangled with the quantized gravitational degrees of freedom and yields information concerning the initial formation of the black hole.

Acknowledgments

This work was partially supported by the JSPS Summer Program and the National Science Foundation under grant numbers OISE-0913132 (PDN), CMS-0404031 and DMR-0804477 (MPB). PDN thanks W G Brown for helpful discussions and H Yamaguchi and the NTT Basic Research Laboratories, where part of this work was carried out, for their hospitality and support.

References

[1] Hawking S W 1974 Black hole explosions *Nature* **248** 30
[2] Hawking S W 1975 Particle creation by black holes *Commun. Math. Phys.* **43** 199
[3] Hartle J B and Hawking S W 1976 Path-integral derivation of black-hole radiance *Phys. Rev.* D **13** 2188
[4] Boulware D G 1976 Hawking radiation and thin shells *Phys. Rev.* D **13** 2169
[5] Gibbons G W and Hawking S W 1977 Action integrals and partition functions in quantum gravity *Phys. Rev.* D **15** 2752
[6] Parentani R 2000 Hawking radiation from feynman diagrams *Phys. Rev.* D **61** 27501

[7] Bombelli L, Koul R K, Lee J and Sorkin R D 1986 A quantum source of entropy for black holes *Phys. Rev.* D **34** 373
[8] Srednicki M 1993 Entropy and area *Phys. Rev. Lett.* **71** 666
[9] Eisert J, Cramer M and Plenio M B 2010 Colloquium: area laws for the entanglement entropy *Rev. Mod. Phys.* **82** 277–306
[10] Aharanov Y, Casher A and Nussinov S 1987 The unitary puzzle and planck mass stable particles *Phys. Lett.* B **191** 51
[11] Giddings S B 1992 Black holes and massive remnants *Phys. Rev.* D **46** 1347
[12] Hawking S W 1988 Wormholes in spacetime *Phys. Rev.* D **37** 904
[13] Frolov V P, Markov M A and Mukhanov V F 1990 Black holes as possible sources of closed and semiclosed worlds *Phys. Rev.* D **41** 383
[14] Page D N 1993 Information in black hole radiation *Phys. Rev. Lett.* **71** 3743
[15] Parikh M K and Wilczek F 2000 Hawking radiation as tunneling *Phys. Rev. Lett.* **85** 5042
[16] Hawking S W 2005 Information loss in black holes *Phys. Rev.* D **72** 084013
[17] Terno D R 2005 From qubits to black holes: entropy, entanglement and all that *Int. J. Mod. Phys.* D **14** 2307
[18] Jacobson T A 1995 Thermodynamics of spacetime: the einstein equation of state *Phys. Rev. Lett.* **75** 1260
[19] Carlip S 2008 Is quantum gravity necessary? *Class. Quantum Gravity* **25** 154010
[20] Dicke R H 1953 Coherence in spontaneous radiation processes *Phys. Rev.* **93** 99
[21] Mollow B R and Glauber R J 1967 Quantum theory of parametric amplification. I *Phys. Rev.* **160** 1076
[22] Travis M and Cummings F W 1968 Exact solutions for an *n*-molecule-radiation-field Hamiltonian *Phys. Rev.* **170** 379
[23] Tucker J and Walls D F 1969 Quantum theory of the traveling-wave frequency converter *Phys. Rev.* **178** 2036
[24] Walls D F and Barakat R 1970 Quantum-mechanical amplification and frequency coonversion with a trilinear Hamiltonian *Phys. Rev.* A **1** 446
[25] Lu E Y C 1973 Quantum theory of nonlinear optical processes with time-dependent pump amplitude and phase: frequnecy conversion *Phys. Rev.* A **8** 1053
[26] Agrawal G P and Mehta C L 1974 Dynamics of parametric processes with a trilinear Hamiltonian *J. Phys. A: Math. Gen.* **7** 607
[27] McNeil K J and Gardiner C W 1983 Quantum statistics of parametric oscillation *Phys. Rev.* A **28** 1560
[28] Gerlach U H 1976 The mechanism of blackbody radiation from an incipient black hole *Phys. Rev.* D **14** 1479
[29] Barnett S M and Knight P L 1985 Thermofield analysis of squeezing and statistical mixtures in quantum optics *J. Opt. Soc. Am.* B **2** 467
[30] Yurke B and Potasek M 1987 Obtainment of thermal noise from a pure state *Phys. Rev.* A **36** 3464
[31] Boyd R W 2003 *Nonlinear Optics* 2nd edn (New York: Academic)
[32] Traux D R 1985 Baker–Campbell–Hausdorff relations and unitarity of SU(2) and SU(1,1) squeeze operators *Phys. Rev.* D **31** 1988
[33] Fuentes-Schuller I and Mann R B 2005 Alice falls into a black hole: entanglement in noninertial frames *Phys. Rev. Lett.* **95** 120404
[34] Walls D F and Milburn G J 2008 *Quantum Optics* 2nd edn (Berlin: Springer)
[35] Kibble T W B and Randjbar-Daemi S 1980 Non-linear coupling of quantum theory and classical gravity *J. Phys. A: Math Gen.* **13** 141
[36] Horowitz G T 1980 Semiclassical relativity: the weak-field limit *Phys. Rev.* D **21** 1445
[37] Anselmi D 2007 Renormalization and causality violations in classical gravity coupled with quantum matter *J. High Energy Phys.* **1** 62
[38] Unruh W G 1984 Steps toward a quantum theory of gravity *Quantum Theory of Gravity: Essays in Honor Of the 60th Birthday if Bryce S. De Witt* (Bristol: Hilger)
[39] Manley J M and Rowe H E 1956 Some general properties of nonlinear elements—Part I. General energy relations *Proc. of IRE* **44** 904
[40] Yurke B, McCall S L and Klauder J R 1986 SU(2) and SU(1,1) interferometers *Phys. Rev.* A **33** 4033

[41] Brif C 1996 Coherent states for quantum systems with a trilinear boson Hamiltonian *Phys. Rev.* A **54** 5253
[42] Mathur S D 2009 The information paradox: a pedagogical introduction *Class. Quantum Gravity* **26** 224001
[43] Nielson M A and Chuang I L 2000 *Quantum Computation and Quantum Information* (Cambridge: Cambridge University Press)
[44] Page D N 1993 Average entropy of a subsystem *Phys. Rev. Lett.* **71** 1291
[45] Popescu S, Short A J and Winter A 2006 Entanglement and the foundations of statistical mechanics *Nat. Phys.* **2** 754
[46] Drobný G and Bužek V 1994 Fundamental limit on energy transfer in K-photon down-conversion *Phys. Rev.* A **50** 3492
[47] Groisman B, Popescu S and Winter A 2005 Quantum, classical, and total amount of correlations in a quantum system *Phys. Rev.* A **72** 032317